ATMOSPHERIC DENSITY ESTIMATION FOR IMPROVED ORBIT DETERMINATION AND CONJUNCTION ASSESSMENT

David Gondelach[(1)], **Srinivas Setty**[(1)], **Christoph Bamann**[(1)], **and Paul Cefola**[(2)]

[(1)] *Vyoma GmbH, Eckhardtstraße 28, D-64289 Darmstadt, Germany, Email: {david.gondelach,srinivas.setty,christoph.bamann}@vyoma.space*
[(2)] *State University of New York at Buffalo, Amherst, NY, USA, Email: paulcefo@buffalo.edu*

ABSTRACT

Accurate atmospheric densities are required for accurate orbit determination and prediction in Low-Earth orbits. In this paper the accuracy of orbit determination using densities estimated using a reduced-order density model and two-line element (TLE) data is assessed. The assessment is carried out by comparing orbit determination and prediction results obtained using different densities. For this, Swarm A's orbit is determined in January 2020 using TLE-estimated densities, NRLMSISE-00 modelled densities and JB2008 modelled densities and precise Swarm densities and the orbit fits are compared against Swarm ephemeris. We find improved orbit determination and estimated ballistic coefficient accuracy using TLE-estimated density compared to NRLMSISE-00 and JB2008 modeled densities. The orbit fits together with predicted densities also showed improved orbit predictions.

Keywords: atmospheric density estimation; orbit determination; orbit prediction.

1. INTRODUCTION

Accurate knowledge of the orbits of all Earth-orbiting objects is required to enable space traffic management for safe and sustainable space operations. However, due to the limited accuracy of dynamical models and orbital tracking data, orbit estimates are often not sufficiently accurate to avoid the problem of probability dilution in satellite conjunction analysis [1]. Atmospheric drag is the largest source of error in orbit determination and prediction for low Earth orbits. Most of the uncertainty stems from inaccurate knowledge of atmospheric density [17]. The uncertainties in the density are due to errors in both the model and the input, such as space weather indices. For orbit determination and short-term orbit prediction ($<$2 days) errors due to model inaccuracy tend to dominate. Whereas errors due to inputs become dominant for longer orbit prediction when predicted space weather data are used. Therefore, the accuracy of orbit determination can be improved by reducing the error of density estimates. This can be achieved by calibrating density models or by estimating thermospheric densities directly using orbital tracking data. Such approaches can significantly reduce the bias and uncertainty of atmospheric densities.

The Jacchia-Bowman-HASDM-2009 (JBH09) is the atmospheric density model operationally used by the US Space Force Combined Space Operations Center for catalogue maintenance and conjunction assessment. JBH09 uses tracking data of 80-90 objects and some high precision data to compute corrections to the JB2008 model every 3 hours [20, 2]. It improves the accuracy of orbit predictions up to 72 hours by 20-45%. Also, two-line element (TLE) data, which is generated using tracking data from the United States Space Surveillance Network, has been used by various authors to estimate densities [5, 24, 19, 7, 10]. Yurasov et al. [24, 25] showed improvements in ballistic coefficient estimates and re-entry predictions using density corrections for the NRLMSISE-00 model obtained using TLE data.

Recently, a new technique for density estimation and prediction was developed by deriving and applying reduced-order models (ROMs) for the thermospheric density [14, 16]. These ROMs have been used to accurately estimate the global thermospheric density through data assimilation of density and orbital data using Kalman filters [15, 10, 11]. Density estimation was demonstrated by assimilating accelerometer-derived density measurements [15], TLE data [10] and radar and GPS tracking data [11]. In particular, it was shown that density estimates based on TLE data are more accurate than the JB2008 and NRLMSISE-00 models, when these densities were compared against CHAMP, GRACE and SWARM precise densities. Moreover, the technique allows for uncertainty quantification of the density estimates as well as prediction of densities and their uncertainty [9].

In this paper, we assess the orbit determination accuracy using TLE-estimated densities obtained with reduced-order models. First, we estimate thermospheric densities using TLE data and quantify the error in the estimated density by comparison against accurate density data. Then the densities are used for orbit determination and the accuracy of resulting orbit solution is compared against orbit fits obtained by using empirical density models. In addition, because fitted ballistic coefficients can soak up errors in the atmospheric density, we also compare the statistics of series of estimated ballistic coefficients obtained using estimated and modelled densities. Finally, the accuracy of orbit predictions is assessed.

2. DENSITY MODELING AND ESTIMATION

In previous work, ROMs for the thermospheric mass density have been developed to enable real-time estimation and forecasting of the global thermospheric density [14, 16, 15, 10, 11]. In this work we use a ROM based on JB2008 density data that was developed in previous work [10]. A brief overview of the reduced-order modeling technique and model characteristics is provided below. More information can be found in [10].

2.1. Reduced-order modeling

The main idea of reduced-order modeling is to reduce the dimensionality of the state space while retaining maximum information. In our case, the full state space consists of the neutral mass density values on a dense uniform grid in latitude, local solar time and altitude with dimensions 20 by 24 by 36 (in total 17280 points). The goal is to develop an efficient and accurate model for the evolution of the density over time. First, to reduce the dimension of the state space we employed Proper Orthogonal Decomposition (POD). Second, we derived a linear dynamic model that accounts for the effect of space weather by applying Dynamic Mode Decomposition with control (DMDc).

2.1.1. Proper orthogonal decomposition

Order reduction using POD is achieved by projecting the high-dimensional system onto a set of a small number of basis functions or spatial modes. These spatial modes are computed such that the dominant characteristics of the system are captured by the first r modes. Consider the variation $\tilde{\mathbf{x}}$ of the neutral mass density $\mathbf{x}$ with respect to the mean value $\bar{\mathbf{x}}$:

$$\tilde{\mathbf{x}}(\mathbf{s},t) = \mathbf{x}(\mathbf{s},t) - \bar{\mathbf{x}}(\mathbf{s}) \tag{1}$$

where $\mathbf{s}$ is the spatial grid. A significant fraction of the variance $\tilde{\mathbf{x}}$ can be captured by the first r principal spatial modes:

$$\tilde{\mathbf{x}}(\mathbf{s},t) \approx \sum_{i=1}^{r} c_i(t)\Phi_i(\mathbf{s}) \tag{2}$$

where Φ_i are the spatial modes and c_i are the corresponding time-dependent coefficients. The spatial modes Φ are computed using a SVD of the snapshot matrix $\mathbf{X}$ that contains $\tilde{\mathbf{x}}$ for different times:

$$\mathbf{X} = [\tilde{\mathbf{x}}_1 \quad \tilde{\mathbf{x}}_2 \quad \cdots \quad \tilde{\mathbf{x}}_m] = \mathbf{U}\boldsymbol{\Sigma}\mathbf{V}^\top \tag{3}$$

where m is the number of snapshots. The spatial modes Φ are given by the left singular vectors (the columns of $\mathbf{U}$). The state reduction is achieved using a similarity transform:

$$\mathbf{z} = \mathbf{U}_r^{-1}\tilde{\mathbf{x}} = \mathbf{U}_r^\top\tilde{\mathbf{x}} \tag{4}$$

where $\mathbf{U}_r$ is a matrix with the first r POD modes and $\mathbf{z}$ is our reduced-order state that contains the corresponding time-dependent coefficients. Projecting $\mathbf{z}$ back to the full space gives approximately $\tilde{\mathbf{x}}$ that allows us to compute the density:

$$\mathbf{x}(\mathbf{s},t) \approx \mathbf{U}_r(\mathbf{s})\,\mathbf{z}(t) + \bar{\mathbf{x}}(\mathbf{s}) \tag{5}$$

More details on POD can be found in [14].

2.1.2. Dynamic Mode Decomposition with control

The atmospheric density depends strongly on the space weather conditions. Therefore, to predict the future density, we look for a function that takes the current state $\mathbf{z}_k$ and space weather inputs $\mathbf{u}_k$ and returns the future state:

$$\mathbf{z}_{k+1} = \mathbf{f}(\mathbf{z}_k, \mathbf{u}_k) \tag{6}$$

where $\mathbf{z}_k$ is the reduced-state at epoch k: $\mathbf{z}_k = \mathbf{U}_r^\top\tilde{\mathbf{x}}_k$.

Dynamic Mode Decomposition with control (DMDc) enables us to derive a linear dynamical system that considers exogenous inputs:

$$\mathbf{z}_{k+1} = \mathbf{A}\mathbf{z}_k + \mathbf{B}\mathbf{u}_k \tag{7}$$

The dynamic matrix $\mathbf{A}$ and input matrix $\mathbf{B}$ can be estimated from output data, or snapshots, $\mathbf{z}_k$, rearranged into time-shifted data matrices. Let $\mathbf{Z}_1$ and $\mathbf{Z}_2$ be the time-shifted matrix of snapshots such that:

$$\mathbf{Z_1} = [\mathbf{z}_1 \quad \mathbf{z}_2 \quad \cdots \quad \mathbf{z}_{m-1}] \tag{8}$$
$$\mathbf{Z_2} = [\mathbf{z}_2 \quad \mathbf{z}_3 \quad \cdots \quad \mathbf{z}_{m}] \tag{9}$$
$$\boldsymbol{\Upsilon} = [\mathbf{u}_1 \quad \mathbf{u}_2 \quad \cdots \quad \mathbf{u}_{m-1}] \tag{10}$$

where m is the number of snapshots and $\boldsymbol{\Upsilon}$ contains the inputs corresponding to $\mathbf{Z}_1$. Since $\mathbf{Z}_2$ is the time evolution of $\mathbf{Z}_1$, they are related through Eq. (7) such that:

$$\mathbf{Z}_2 = \mathbf{A}\mathbf{Z}_1 + \mathbf{B}\boldsymbol{\Upsilon} \tag{11}$$

Given $\mathbf{Z}_1$ and $\mathbf{Z}_2$, we can estimate matrices $\mathbf{A}$ and $\mathbf{B}$ in least-squares sense and obtain a linear reduced-order model (Eq. 7) that corresponds to the fixed timestep T used for the snapshots. For estimation we require continuous information about the density and therefore need a continuous dynamical model:

$$\dot{\mathbf{z}} = \mathbf{A}_c\mathbf{z} + \mathbf{B}_c\mathbf{u} \tag{12}$$

where $\mathbf{A}_c$ and $\mathbf{B}_c$ are the continuous-time dynamic and input matrices, respectively. The continuous-time matrices are obtained by converting the discrete-time matrices using the following relation [6]:

$$\begin{bmatrix} \mathbf{A}_c & \mathbf{B}_c \\ \mathbf{0} & \mathbf{0} \end{bmatrix} = \log\left(\begin{bmatrix} \mathbf{A} & \mathbf{B} \\ \mathbf{0} & \mathbf{I} \end{bmatrix}\right)/T \tag{13}$$

where T is the sample time, i.e. the snapshot resolution. Now using Eqs. (4) and (5) we can map between the full and reduced space and Eq. (12) allows us to predict the density.

2.2. Density estimation

The neutral mass density is estimated through the assimilation of TLE data in the ROM model. This is achieved by simultaneously estimating the ROM state $\mathbf{z}$ and the orbit and ballistic coefficient (BC) of objects using an unscented Kalman filter (UKF). Orbital states derived from TLE data are used as measurement data.

For estimation, the objects' orbits are expressed in modified equinoctial elements (MEE) (p, f, g, h, k, L). The full state $\mathbf{x}$ that is estimated contains the orbital states and BCs for each object and the reduced-order density state $\mathbf{z}$:

$$\mathbf{x} = \left[p^1, f^1, g^1, h^1, k^1, L^1, BC^1, \quad \dots \quad, BC^n, \quad \mathbf{z}^\top\right]^\top \tag{14}$$

where the superscripts 1 and n refer to the different objects. The measurement data $\mathbf{y}$ for estimation are orbital states derived from the TLE data of the objects. These TLE orbital states are also expressed in MEE.

Starting from an initial guess $\mathbf{x}_0$, the density estimation process is as follows, see Figure 1. The state $\mathbf{x}_{i-1|i-1}$ and corresponding covariance $\mathbf{P}_{i-1|i-1}$ are propagated using the orbital dynamics $\mathbf{F}$ (see next section) and ROM model (see Eq. (12)) to the next measurement epoch i through an unscented transform. Then the state and covariance are updated using the measurements $\mathbf{y}_i$ and corresponding measurement noise $\mathbf{R}_i$ to obtain a new state estimate $\mathbf{x}_{i|i}$ and covariance $\mathbf{P}_{i|i}$. Figure 1 shows a diagram of the estimation process, where $\mathbf{u}$ are the space weather inputs and Q is the process noise. The prediction and update of the state covariance $\mathbf{P}$ are not shown for readability. More information about the approach can be found in [10].

By estimating $\mathbf{x}$ over a period of time, we obtain a history of global thermospheric density estimates in the form of a time series of reduced-order density states $\mathbf{z}$. These density estimates can be used for orbit determination. For example, in the future, using the tracking data of a selected set of objects the global density can be estimated. Those densities can be used to perform orbit determination for all tracked objects in LEO for cataloguing and space traffic management. The density estimation and cataloguing processes can run in parallel to obtain densities and maintain the catalogue as soon as new measurements are collected.

2.3. Density prediction

Once we have obtained a density estimate, we can use the dynamic ROM to predict future densities by propagating the estimated reduced-order density state $\mathbf{z}$ forward in time using Eq. (12). From the predicted $\mathbf{z}$, local atmospheric densities can be computed by converting $\mathbf{z}$ to the full space using Eq. (5) and interpolating the density grid. In this work, we use ROM-predicted densities to perform orbit prediction. Here, we assume that the future space weather proxies $\mathbf{u}$ needed for prediction are known, such that errors in the density prediction are due to errors in the initial density state and ROM model but not due to space weather prediction inaccuracies.

3. ORBIT DETERMINATION ASSESSMENT

To assess the accuracy of orbit determination using TLE-estimated densities, we compare orbit determination (OD) results obtained using TLE-estimated, empirically-modelled and precise densities. For this, we determine the orbit of ESA's Swarm A satellite in January 2020 when it was flying at an altitude of 430 km. To clearly observe the effect of density on the OD result, we minimize orbit fit errors due to other sources as much as possible by using a high-accuracy force model and highly-accurate measurement data, namely Swarm ephemeris data.

Force model The applied force model includes:

- Geopotential acceleration computed using the EGM2008 model, up to degree and order 70 for the harmonics;
- Cannonball solar radiation pressure with cylindrical shadow model and cannonball model;
- Third body perturbations by Sun and Moon;
- Atmospheric drag considering a rotating atmosphere for computing the velocity relative to the atmosphere and constant ballistic coefficient.

A cannonball drag and solar radiation pressure model are assumed, because these are practical models for orbit determination of objects with unknown properties or attitude, such as space debris. Solid Earth and ocean tides, Earth albedo and radiation, relativistic effects, wind in the upper thermosphere and changes in attitude or drag coefficient are not considered.

Measurement data As measurement data we use Swarm precise dynamic position ephemeris that have an uncertainty of 10 cm in 3D position [21]. We have one position measurement every 30 seconds.

Due to the use of a highly accurate force model and measurements, the main source of error in the OD solution is expected to be due to inaccurate atmospheric densities.

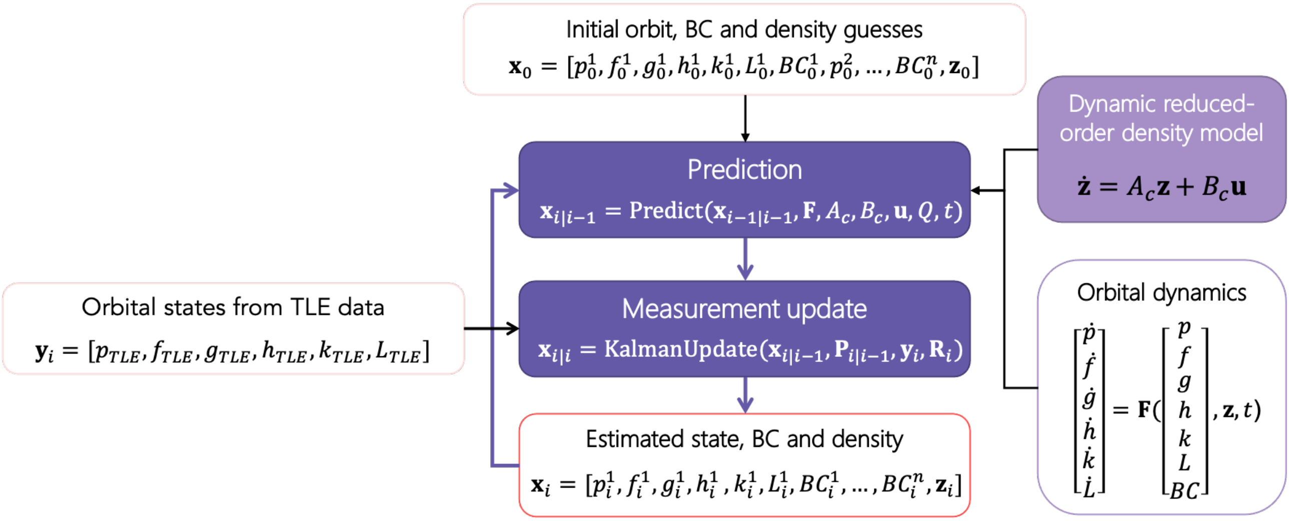

Figure 1: Flowchart of density estimation via TLE data assimilation. The orbital states $(p^i, f^i, g^i, h^i, k^i, L^i)$ and BCs (BC^i) of the objects and the reduced-order density state $\mathbf{z}$ are estimated simultaneously using orbital states from TLE data. The orbital dynamics and the ROM are used for prediction. An unscented Kalman filter is applied for estimation.

To verify this, we perform OD using precise densities derived from Swarm GPS data [23], see next section.

Orbit determination The OD is performed by estimating the state, ballistic coefficient ($BC = C_d A/m$) and SRP coefficient (coefficient ($SRPC = C_r A/m$) using batch least-squares estimation. We use a fit span of five days and the OD solution epoch is in the middle of the OD window.

Accuracy assessment The accuracy of the OD results is assessed by analysing the root-mean-square (RMS) position residuals with respect to the measurement data (i.e. Swarm ephemeris) in radial, transverse and normal directions. In addition, the estimated BCs are examined and compared against the BC estimated using precise density data and the theoretical BC value. In addition, starting from the resulting orbit fits, we predict orbits two days into future to assess the orbit prediction accuracy.

4. DENSITY DATA

The TLE-estimated density used in this work were estimated using the ROM-JB2008 model and TLE data of 20 objects in January 2020 (the perigee altitude of the 20 objects was between 300 and 523 km altitude). The objects and settings used for estimation are described in detail in [11]. To assess the accuracy of the TLE-estimated densities, we compared them against precise densities along Swarm A's orbit derived from GPS data by Van den IJssel et al. [23]. These precise Swarm A densities have a (conservatively-estimated) relative uncertainty of 19% in *local* density during low solar activity, while the *orbit-average* densities have a much lower uncertainty.

Figure 2a shows the precise Swarm A orbit-averaged density and densities estimated using TLE data and according to the JB2008 [3] and NRLMSISE-00 [18] models, while Figure 2b and Table 1 show the error in estimated and modeled densities in January 2020. The TLE-estimated densities are more accurate than the empirically modelled densities as they have both a smaller bias and smaller standard deviation. A constant bias in the density can be compensated during OD by fitting the BC. However, if the error is changing over time (see Figure 2b) then this is expected to affect the orbit fit accuracy.

Table 1: Accuracy of TLE-estimated and modelled densities along SWARM A's orbit in January 2020. The numbers show the mean μ, standard deviation σ and root-mean-square (RMS) of the error in orbit-averaged and daily-average density as percentage of true densities [11].

Density	Density error [%]					
	Orbit-average			Daily-average		
	μ	σ	RMS	μ	σ	RMS
NRLMSISE-00	80.5	24.1	84.0	79.8	21.8	82.6
JB2008	18.8	20.3	27.6	18.6	12.3	22.1
TLE-estimated	2.3	11.3	11.5	2.1	8.6	8.7

5. RESULTS

5.1. Orbit determination accuracy

Using each type of density data, we performed 21 ODs (each shifted by one day) between January 3 and 28, 2020. Figure 3 shows the average post-fit RMS position residual (average of the 21 orbit fits) for each density data type. As expected, using the precise Swarm density data provides most accurate orbit fits. This suggests that the higher errors in the orbit fits obtained using other den-

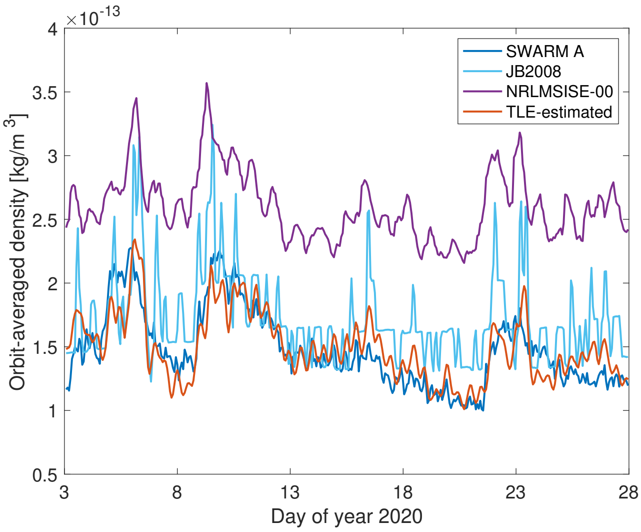

(a) Orbit-averaged density

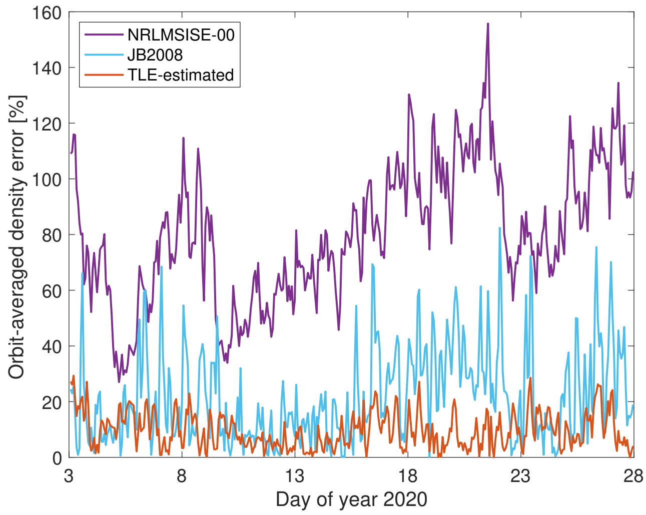

(b) Orbit-averaged density error

Figure 2: Orbit-averaged density and error along SWARM A's orbit estimated using TLE data and according to SWARM A data and JB2008 and NRLMSISE-00 models from January 3 to 28, 2020 [11].

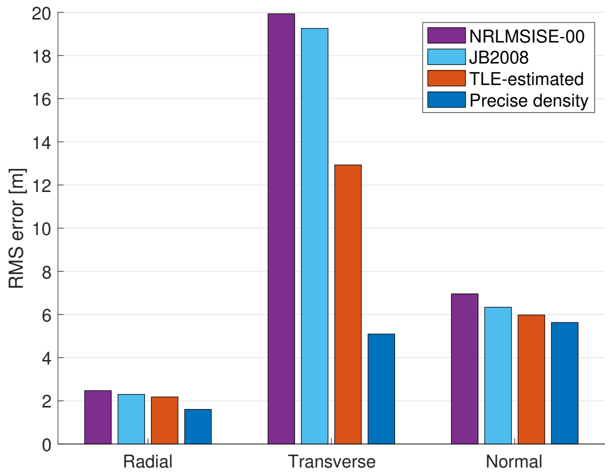

Figure 3: Average RMS position residual of orbit fits w.r.t. Swarm-A ephemeris in radial, transverse and normal direction.

sity data are due to errors in the atmospheric density. The fact that the post-fit residuals using precise density are not zero can be contributed to neglecting perturbations (e.g. solid Earth tides) and inaccurate force modelling (e.g. we assumed a constant ballistic coefficient and did not consider atmospheric winds, while local variations in the BC and winds can be expected).

The orbit fits obtained using TLE-estimated density are on average more accurate than those obtained using the JB2008 and NRLMSISE-00 densities. Table 2 shows that the improvement is mainly in the transverse (i.e. in-track) direction, in which the RMS residual is on average about 30% lower compared to using empirically modeled densities.

5.2. Estimated ballistic coefficient

The BC was estimated during OD to obtain accurate orbit fits. Figure 4 and Table 5 show that the BC estimated using the TLE-estimated density are close to the BC estimated using precise density data. In addition, the variation in the estimated BC values obtained using TLE-estimated density is smaller than the BC variation when using JB2008 or NRLMSISE-00 densities (the true BC is expected to be near-constant as shown by the BCs estimated using precise density data). Comparing the estimated BCs (Figure 4) and daily-averaged density error (Figure 5) shows that the variation in the BC is opposite but proportional to the density error. This indicates that the estimated BCs compensate for the error in the atmospheric density.

These results show that one can obtain improved BC estimates using TLE-estimated densities. This is particularly important when one has limited tracking data for an object. Using accurate density data one can obtain an accurate estimate for the BC with a limited number of

Table 2: Accuracy of orbit determination and prediction.

Density	Post-fit RMS residual [m]			1-day prediction error [m]			2-day prediction error [m]		
	Radial	Transverse	Normal	Radial	Transverse	Normal	Radial	Transverse	Normal
NRLMSISE-00	2.5	19.9	7.0	5.3	170.9	13.6	6.7	367.2	16.7
JB2008	2.3	19.3	6.3	4.8	150.0	13.8	6.2	336.0	17.1
TLE-estimated	2.2	12.9	6.0	5.1	104.4	13.1	6.7	261.7	16.4
Precise density	1.6	5.1	5.6	3.8	23.7	12.3	4.9	44.9	15.3

Table 3: Average estimated ballistic coefficients and percentage variation in estimated BCs.

Density	Mean BC [m^2/kg]	BC variation [%]
NRLMSISE-00	0.00453	41
JB2008	0.00675	32
TLE-estimated	0.00792	22
Precise density	0.00792	3.5

ODs, whereas using empirically modelled densities the estimated BC may be strongly biased. As the density bias may change over time, the biased BC can result in inaccurate orbit predictions.

Finally, March et al. [13] estimated Swarm's drag coefficient using high-fidelity geometry models and found a C_d of 3.2, assuming a reference area of 1 m^2. Using a satellite mass of approximately 400 kg, we then obtain a BC of 0.008 m^2/kg. This theoretical value is very close to the average BC estimated using precise and TLE-estimated densities, which give additional confidence that the BC estimate is accurate[1].

5.3. Orbit prediction accuracy

Starting from the orbit fits obtained using OD, we predict the orbits two days into the future to assess the resulting orbit prediction accuracy. We assume perfect knowledge of the future space weather. This mean that orbit prediction errors are due to errors in both the OD result and the density models. In case of TLE-estimated density, we use the ROM to predict the future density. Figure 6 shows the error in daily-averaged density predicted using the ROM model. The errors in the predicted density grow with time but on average remain smaller than errors in the JB2008 densities for this period.

Figure 7 and Table 2 show the orbit prediction accuracy using ROM-predicted, empirically-modelled and precise Swarm densities starting from their respective orbit fits. As expected, the orbit predictions after 1 and 2 days using

[1]It should be noted that the precise Swarm densities were computed using the high-fidelity geometry models developed by March et al. [13], so their values are not independent.

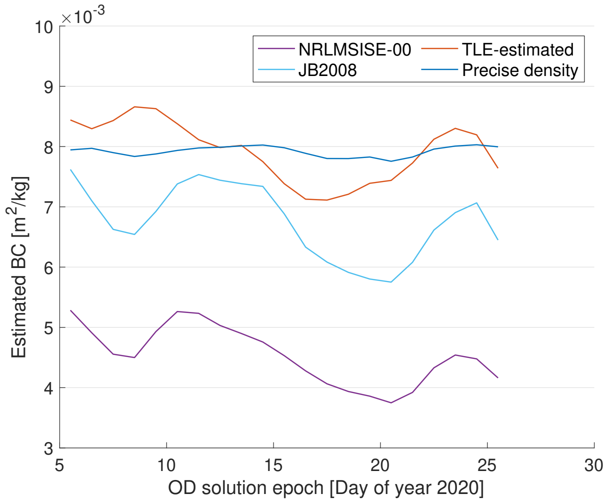

Figure 4: Estimated ballistic coefficients using different densities during OD.

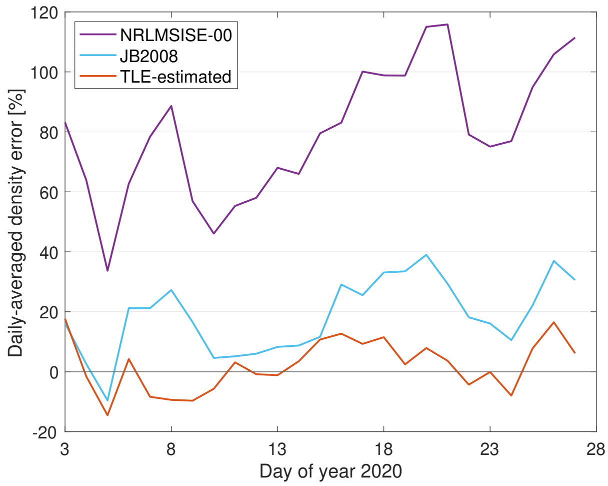

Figure 5: Error in daily-averaged density along SWARM A's orbit estimated using TLE data and according to JB2008 and NRLMSISE-00 models from January 3 to 28, 2020.

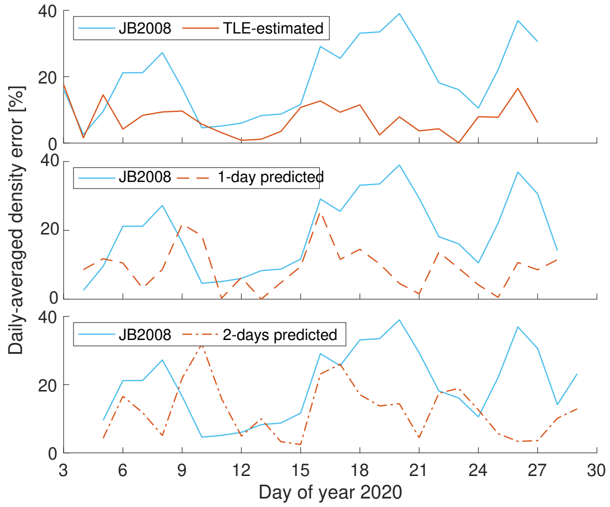

Figure 6: Error in daily-averaged density estimated using TLE data and predicted using ROM for 1 and 2 days into the future. Error in JB2008 densities is shown as reference.

precise densities are most accurate. The predictions starting from the TLE-estimated densities are more accurate than using empirically modelled densities. This shows that densities estimated and predicted using a ROM can improve both orbit determination and prediction.

6. DISCUSSION

The results obtained in the previous section show that by using TLE-estimated densities, which are more accurate than empirically modeled densities, one can improve orbit determination. In addition, the improved orbit fits resulted in improved orbit prediction while the future densities were computed using the ROM density model. Such improved orbit predictions are very valuable for conjunction assessment to obtain better probability of collision estimates [12].

The results obtained here are for one object for one month during solar minimum. More extensive analysis of the orbit determination and prediction accuracy will be carried out over longer periods of time and during different solar activity to obtain statistics of the OD improvement using TLE-estimated densities, similar to the studies on error reduction using HASDM [4, 20].

In this work we assumed perfect knowledge of the future space weather, which is not the case in practice. In particular during space weather events, the predicted solar and geomagnetic activity can be erroneous and these errors can dominate the density model errors. The effect of space weather forecasting errors on the orbit prediction accuracy was studied by e.g. [8] and is part of future research. Still, regardless of the accuracy of space weather forecasts, improved orbit determination is beneficial for orbit prediction accuracy.

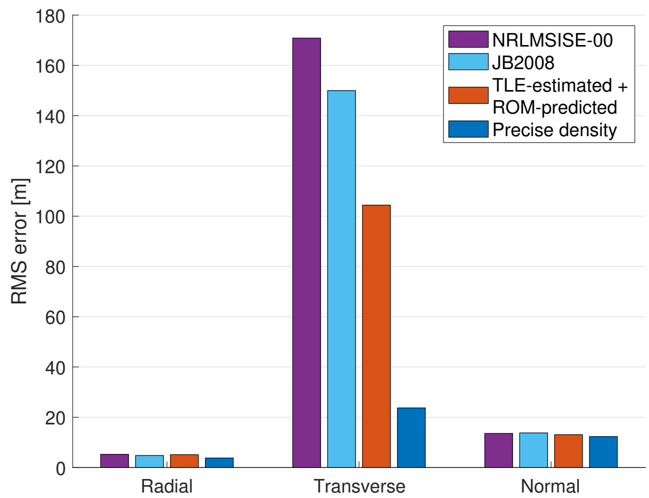

(a) 1-day prediction

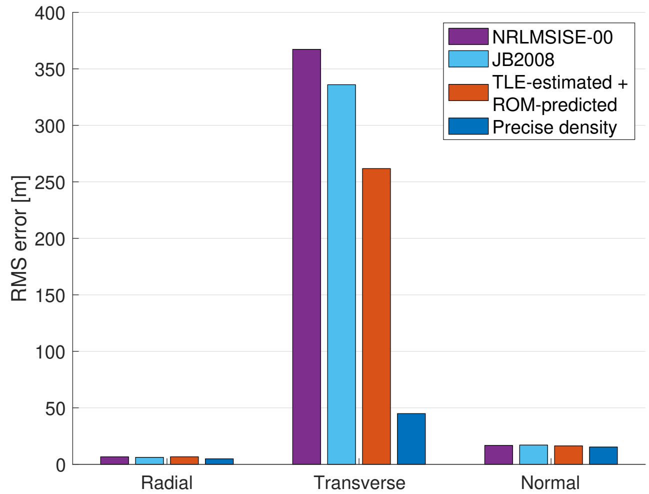

(b) 2-days prediction

Figure 7: Position error (RMSE over one orbit) after 1 and 2 days prediction using different densities starting from OD result.

7. CONCLUSIONS

Atmospheric density models for computing drag forces on satellites are a major source of inaccuracy in trajectory predictions for low-perigee satellites. Using a reduced-order density model and two-line element data we obtained improved density estimates with respect to empirical density models. These TLE-estimated densities were used to perform orbit determination and the accuracy of the resulting orbit fits and predictions were assessed.

For the assessment, the orbit of the Swarm A satellite was estimated using an accurate force model and precise position data as measurements using TLE-esimated, NRMSISE-00 and JB2008 and precise densities. The accuracy of the orbit fits using TLE-esimated densities were found to be more accurate then orbit solutions obtained using NRMSISE-00 and JB2008 modeled densities. Moreover, the estimated BCs are more accurate and show less variation over time compared to BCs estimated using empirical densities. Finally, also orbit predictions using densities predicted by the reduced-order density model were on average more accurate. These findings show that orbit determination and prediction can be improved using densities estimated with TLE data.

The analysis in this work was carried out for one month during low solar activity. This assessment will be extended in future work to analyse the performance during different space weather conditions and for different orbits. In addition, by using more accurate tracking data, such as radar or GPS tracking data, better density estimates can be obtained to achieve even better OD and orbit prediction results [11]. Furthermore, the predictive capability of the ROM can be improved, e.g. using non-linear machine-learning techniques [22], to obtain more accurate density forecasts.

ACKNOWLEDGMENTS

David Gondelach would like to thank Dr. Richard Linares at MIT, Cambridge, USA, for his guidance on the topic. The SWARM densities used in this work were derived by [23]. The Swarm densities and ephemeris can be obtained from the Swarm Data Access: https://swarm-diss.eo.esa.int/#swarm/Level2daily/Entire_mission_data under DNS/POD and POD/RD, respectively. The NRLMSISE-00 and JB2008 models used in this work can be found on https://www.brodo.de/space/nrlmsise and http://sol.spacenvironment.net/jb2008/code.html, respectively. The space weather proxies were obtained from http://celestrak.com/SpaceData/ and http://sol.spacenvironment.net/jb2008/indices.html. Two-line element data was downloaded from https://www.space-track.org.

REFERENCES

1. S. Alfano. Relating position uncertainty to maximum conjunction probability. *The Journal of the Astronautical Sciences*, 53(2):193–205, 2005.
2. B. R. Bowman and W. K. Tobiska. Thermospheric density analyses project HASDM. In *CEDAR-GEM Challenge Meeting, 2014 Space Weather Workshop, Boulder, CO*, 2014.
3. B. R. Bowman, W. K. Tobiska, F. Marcos, C. Huang, C. Lin, and W. Burke. A new empirical thermospheric density model JB2008 using new solar and geomagnetic indices. In *Proceedings of the AIAA/AAS Astrodynamics Specialist Conference and Exhibit, August 18-21, Honolulu, HI*, 2008.
4. S. Casali and W. Barker. Dynamic calibration atmosphere (DCA) for the high accuracy satellite drag model (HASDM). In *AIAA/AAS Astrodynamics Specialist Conference and Exhibit, Monterey, CA*, 2002. doi: https://doi.org/10.2514/6.2002-4888.
5. P. J. Cefola, R. J. Proulx, A. I. Nazarenko, and V. S. Yurasov. Atmospheric density correction using two line element sets as the observation data. *Advances in the Astronautical Sciences*, 116:1953–1978, 2004.
6. R. A. DeCarlo. *Linear Systems: A State Variable Approach with Numerical Implementation*. Prentice-Hall, Inc., Upper Saddle River, NJ, USA, 1989. ISBN 0-13-536814-6.
7. E. Doornbos, H. Klinkrad, and P. Visser. Use of two-line element data for thermosphere neutral density model calibration. *Advances in Space Research*, 41 (7):1115–1122, 2008.
8. J. Emmert, H. Warren, A. Segerman, J. Byers, and J. Picone. Propagation of atmospheric density errors to satellite orbits. *Advances in Space Research*, 59(1):147–165, 2017. ISSN 0273-1177. doi: https://doi.org/10.1016/j.asr.2016.07.036. URL https://www.sciencedirect.com/science/article/pii/S0273117716304355.
9. D. J. Gondelach and R. Linares. Atmospheric density uncertainty quantification for satellite conjunction assessment. In *AIAA Scitech 2020 Forum*, page 0232, 2020. doi: https://doi.org/10.2514/6.2020-0232.
10. D. J. Gondelach and R. Linares. Real-time thermospheric density estimation via two-line element data assimilation. *Space Weather*, 18(2): e2019SW002356, 2020. doi: https://doi.org/10.1029/2019SW002356.
11. D. J. Gondelach and R. Linares. Real-time thermospheric density estimation via radar and gps tracking data assimilation. *Space Weather*, page e2020SW002620, 2021. doi: https://doi.org/10.1029/2020SW002620.
12. M. D. Hejduk and D. E. Snow. The effect of neutral density estimation errors on satellite conjunction serious event rates. *Space Weather*, 16 (7):849–869, 2018. doi: https://doi.org/10.1029/2017SW001720. URL https://agupubs.onlinelibrary.wiley.com/doi/abs/10.1029/2017SW001720.

13. G. March, E. Doornbos, and P. Visser. High-fidelity geometry models for improving the consistency of champ, grace, goce and swarm thermospheric density data sets. *Advances in Space Research*, 63(1): 213–238, 2019.

14. P. M. Mehta and R. Linares. A methodology for reduced order modeling and calibration of the upper atmosphere. *Space Weather*, 15(10):1270–1287, 2017. doi: https://doi.org/10.1002/2017SW001642.

15. P. M. Mehta and R. Linares. A new transformative framework for data assimilation and calibration of physical ionosphere-thermosphere models. *Space Weather*, 16(8):1086–1100, 2018. doi: https://doi.org/10.1029/2018SW001875.

16. P. M. Mehta, R. Linares, and E. K. Sutton. A quasi-physical dynamic reduced order model for thermospheric mass density via hermitian space-dynamic mode decomposition. *Space Weather*, 16 (5):569–588, 2018. doi: https://doi.org/10.1029/2018SW001840.

17. National Research Council. *Continuing Kepler's Quest: Assessing Air Force Space Command's Astrodynamics Standards*. National Academies Press, 2012.

18. J. Picone, A. Hedin, D. Drob, and A. Aikin. NRLMSISE-00 empirical model of the atmosphere: Statistical comparisons and scientific issues. *J. Geophys. Res.*, 107(A12):1468, 2002.

19. J. Picone, J. Emmert, and J. Lean. Thermospheric densities derived from spacecraft orbits: Accurate processing of two-line element sets. *Journal of Geophysical Research: Space Physics*, 110(A3), 2005.

20. M. F. Storz, B. R. Bowman, M. J. I. Branson, S. J. Casali, and W. K. Tobiska. High accuracy satellite drag model (HASDM). *Advances in Space Research*, 36(12):2497–2505, 2005.

21. Swarm Level 2 Processing System Consortium. Product specification for l2 products and auxiliary products. *Doc. no: SW-DS-DTU-GS-0001*, 2019.

22. H. Turner, M. Zhang, D. Gondelach, and R. Linares. Machine learning algorithms for improved thermospheric density modeling. In F. Darema, E. Blasch, S. Ravela, and A. Aved, editors, *Dynamic Data Driven Applications Systems*, pages 143–151, Cham, 2020. Springer International Publishing. ISBN 978-3-030-61725-7.

23. J. van den IJssel, E. Doornbos, E. Iorfida, G. March, C. Siemes, and O. Montenbruck. Thermosphere densities derived from swarm gps observations. *Advances in Space Research*, 65(7):1758 – 1771, 2020. ISSN 0273-1177. doi: https://doi.org/10.1016/j.asr.2020.01.004.

24. V. S. Yurasov, A. I. Nazarenko, P. J. Cefola, and K. T. Alfriend. Density corrections for the NRLMSIS-00 atmosphere model. In *Proceedings of the AAS/AIAA Space Flight Mechanics Conference, January 23-27, Copper Mountain, CO*, pages 1079–1107, 2005.

25. V. S. Yurasov, A. I. Nazarenko, K. T. Alfriend, and P. J. Cefola. Reentry time prediction using atmospheric density corrections. *Journal of guidance, control, and dynamics*, 31(2):282–289, 2008.